Heliyon 9 (2023) e17872

Contents lists available at ScienceDirect

Heliyon

journal homepage: www.cell.com/heliyon

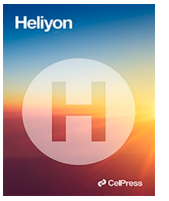

Trimming of sheep spinal cord by waterjet; an experimental study

R. Derakhshan [a], M.T. Ahmadian [b,*], M. Chizari [c], H. Samimiardestani [d]

[a] School of Mechanical Engineering, Sharif University of Technology, Tehran, Iran
[b] School of Mechanical Engineering, Sharif University of Technology, Center of Excellence in Design, Robotic and Automation, Tehran, Iran
[c] School of Physics, Engineering & Computer Sciences, University of Hertfordshire, Hatfield, UK
[d] Otorhinolaryngology Research Center, Department of Otolaryngology-Head and Neck Surgery, Amir-Alam Hospital, Tehran University of Medical Sciences, School of Medicine, Tehran, Iran

ARTICLE INFO

Keywords:
Spinal cord
Waterjet
Meninges layer
Medical operation
Experimental test
Sheep
Surgery
Standard criteria

ABSTRACT

The spinal cord is a structure of nervous tissue that primarily transmits nerve signals from the motor cortex to the body and from the afferent fibers of the sensory neurons to the sensory cortex. It is enveloped by three layers of meninges. Covering provides a supportive framework for the cerebral and cranial vasculature and protects the central nervous system (CNS) from mechanical damage. Surgical operation in the vicinity of the spinal cord is complicated and risky because it exposes it to probably irreversible damage. To reduce the risk of these operations, attempts have been made to remove the tumor using safer methods like waterjet operation. In these methods, the waterjet and spinal cord interaction are inevitable. To secure interaction of operation, a standard development of waterjet criteria is necessary.

In this study, a system of waterjet is designed to perform sheep spinal cord as a tissue with a good resemblance to the human spinal cord. Effects of interaction between waterjet and sheep spinal cord are investigated to define a safe operation threshold. The impact of the liquid density of waterjet on failure criteria of spinal cord surgery is also investigated. Results show that meninges are stiff enough to protect the sheep spinal cord from rupture for pressures up to 8 bar; however internal spinal cord tissue cannot be guaranteed any damage. Three essential parameters represent the spinal cord meninges and spinal cord deformation during the tests. These parameters lead us to provide standard criteria for damage prevention of the spinal cord.

1. Introduction

Spinal cord functions primarily in the transmission of nerve signals from the motor cortex to the body, and from the afferent fibers of the sensory neurons to the sensory cortex. It is also a center for coordinating many reflexes and contains reflex arcs that can independently control reflexes [1]. The spinal cord is the location of groups of spinal interneurons that make up the neural circuits known as central pattern generators. These circuits are responsible for controlling motor instructions for rhythmic movements such as walking. In transverse sections, the spinal cord displays white and the gray matter tissues. Peripherally located, the former contains white matter tracts (ascending and descending myelinated fibers) containing both sensory and motor axons. Centrally located, the latter is characterized by its butterfly-shape that contains gray matter cells (unmyelinated). In the center, there is a central canal that contains cerebrospinal fluids traveling up to the ventricles located in the brain [2].

* Corresponding author.
E-mail address: ahmadian@sharif.edu (M.T. Ahmadian).

https://doi.org/10.1016/j.heliyon.2023.e17872
Received 19 March 2022; Received in revised form 8 May 2023; Accepted 29 June 2023
Available online 8 July 2023

The meninges are the three membranes that envelop the brain and spinal cord and separate them from the walls of their bony cases (skull and vertebral column). Based on their location, meninges are referred to as the cranial meninges which envelop the brain, and spinal meninges which envelop the spinal cord. However, the cranial and spinal meninges are continuous with each other and consist of the same three meningeal layers. From superficial to deep the meninges are the: Dura mater, Arachnoid mater, Pia mater. Dura mater: The outermost layer is the toughest and comprised of dense fibrous tissue, which provides the most protection. The dura mater is the only layer of the meninges that is sensitive to pain. Arachnoid mater: The middle layer is filled with elastic tissues and collagen in a spider web-like structure, which is how this layer gets its name. The cerebrospinal fluid runs beneath the arachnoid mater in the subarachnoid space and above the pia mater. Pia mater: The innermost layer attaches to and closely lines the spinal cord and brain, unlike the looser-fitting arachnoid mater and dura mater on the outside. The pia mater is the thinnest and most delicate of the three meningeal layers. These layers bound three clinically important potential spaces: the epidural, subdural, and subarachnoid spaces. The function of the meninges is to protect the brain and spinal cord from mechanical trauma, to support the blood vessels and to form a continuous cavity through which the cerebrospinal fluid (CSF) passes [2,3]. The optic nerve located in frontal skull base is also ensheathed in meninges [4].

Moreover, it is noticeable that resection of tumors in the vicinity of spinal cord is complicated and risky, because the margins between the intramedullary tumors and normal spinal cord tissue are often unclear [5]. Removing of skull base tumors is also in adjunction of optic and olfactory nerves that exposes them to probable morbidity. Ogawa et al. [6] recently studied on a new technique to remove the hypophysis tumor in the skull base region. This technique was applied by pulsed laser-induced liquid jet (LILJ) system that removes the tumor efficiently and safely without any harm to blood vessels and nerves. Moreover, a study has been published by Nakagawa et al. [7] regarding the safety of using LILJ system, which concluded that water jet is safe in removing lesions on pituitary gland and surrounding area.

Endo et al. [8] studied feasibility of waterjet in dissecting the spinal cord. Waterjet was applied to dissect posterior median sulcus of anesthetized swine spinal cords. Results show that increased strength and exposure time of waterjet led deeper and wider dissections of the spinal cord. They found that waterjet is feasible and reliable option in dissecting the spinal cord. It could possibly achieve both spinal cord dissection and functional preservation.

In another study, Endo et al. [9] use actuator-driven pulsed water jet for resection of brain and spinal cord cavernous malformations. Four patients (2 women and 2 men, mean age 44.5 years) with brain (n = 3) and spinal cord (n = 1) cavernous malformations were enrolled in the study. All surgeries were performed with the aid of the ADPJ (actuator-driven pulsed water jet) system. Postoperative neurological function and radiological findings were evaluated. Results showed that waterjet provided a clear surgical field and enabled surgeons to dissect boundaries between lesions and surrounding brain and spinal cord gliotic tissue. The ADPJ system is a feasible option for cavernous malformation surgery, enabling successful tumor removal and preservation of neurological function.

Considering the importance surgery for intramedullary tumors along with functional preservation of the spinal cord, Endo et al. [10] evaluate the usefulness and safety of water jet dissection in an experimental study as a novel tool in spinal cord surgery. A pulsed water jet was applied to dissect the posterior median sulcus of the spinal cords of seven anesthetized pigs. They concluded that the pulsed water jet is a feasible option for spinal cord dissection. Characteristics of this water jet may help surgeons achieve complete resection of intramedullary tumors along with preserving satisfactory postoperative neurologic functions.

Balak presented two cases where the “quadrantectomy approach”, a sub-category of the unilateral approach, was used for resection of spinal ependymoma and propose a new classification system of the unilateral approach regarding bone drilling and describe the use of a ball-tipped water jet dissector in this procedure. He found that the ball-tipped water jet dissector is a beneficial tool for surgery in the cauda equina region [11]. Furthermore, nowadays, to reduce the risk of operation, more attempts have been made to remove tumor using liquid [12].

One of the main problems for in-vitro experimental investigations is that fresh human specimens are difficult to obtain, and when available such specimens are required in large quantities to overcome the wide scattering effect associated with biological variability [13]. To solve this problem, animal specimens are utilized regularly. Specifically, to provide a model for the human spine, animals such as sheep, goat, pig, calf have been widely used. Such animal specimens are more readily available [14] and show much better homogeneity than do human specimens when selected for breed, sex, age, and weight [15,16]. Sheep in particular are often used as a model for in-vivo studies concerning, for instance, histomorphology of the intervertebral disc [17–19] and biomechanical efficacy of fusion techniques in the lumbar spine [20]. Sheep spines have also been used in vitro to study the initial stabilizing effect of spinal implants in the lumbar [21–23] and cervical regions [24]. Wilke shows sheep and human vertebrae are most similar in the thoracic and lumbar regions [25]. Also, Human spinal cord and meninges have similar structure as sheep’s. Zhang et al. developed an in-vivo indentation test method to measure the force and displacement of indenter on sheep spinal cord with meninges. An equivalent in-vivo Young’s modulus of spinal cord with meninges was then obtained [26].

In the present study, a waterjet system is designed to perform spinal cord. In order to minimize risk of treatment, threshold characteristics of waterjet is provided, to perform safe surgical performance. Effect of liquid’s density of waterjet on failure criteria of spinal cord surgery is also investigated.

To fulfil the objectives of the study, 4 different experimental tests (Tests 1–4) been performed. In Test 1, the uniformity of spinal cord deflection under the waterjet interaction in different directions and along the spinal cord is examined. In Test 2, effects of nozzle diameter, waterjet velocity and fluid’s density on spinal cord deflection is evaluated. In this test, elastic and plastic deformation of spinal cord is also investigated. Since the waterjet is not always perpendicular to spinal cord axis in medical operation, effect of waterjet angle on spinal cord deflection is studied in Test 3. In Test 4, dura mater layer is removed and its deformation under waterjet interaction is analyzed for different nozzles and velocities.

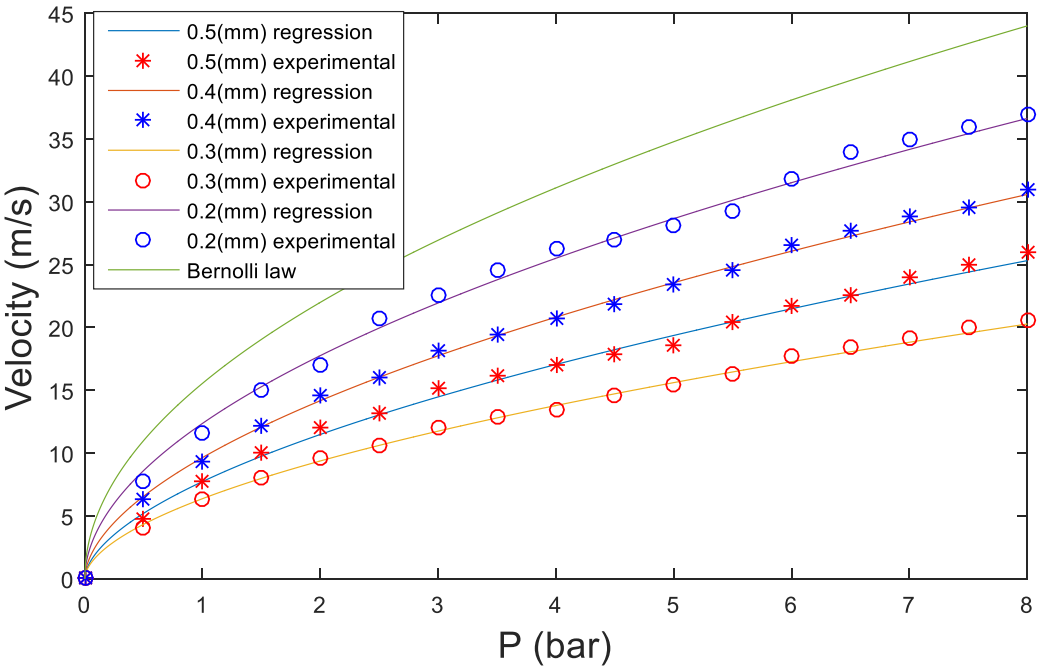

a

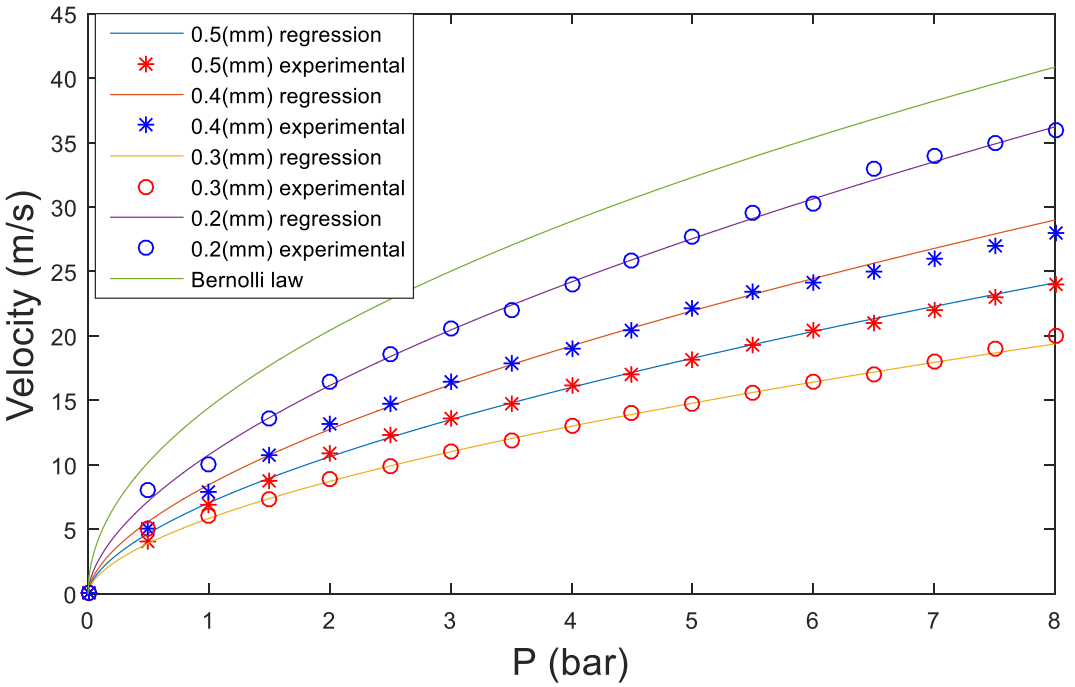

b

Fig. 1. Waterjet velocity calibration on gage pressure: a) for pure water b) for saturated saltwater $\rho \simeq 1000 \mathrm{kg/m^3}$, .

2. Material & methods

2.1. Waterjet apparatus

A waterjet apparatus is designed with different nozzle diameter (0.2, 0.3, 0.4, 0.5 mm) to have different span of waterjet caliber. A controller system is designed to make sure the water pressure remains constant during the test. The controller equipped with a microcontroller which is programmed in C++ to control a solenoid valve and adjust the water pressure. The controller was using a relay as an actuator to adjust the air compressor and maintain the desire water pressure. As the result, waterjet output velocity remains constant and stable during the test.

2.2. Waterjet velocity calibration

In the absent of energy loss, the speed of waterjet can be calculated using Eq. (1) which has been derived from based on Bernoulli's law. Eq. (1) provide pressure between point 1 and point 2.

$$\frac{1}{2}\rho {V_1}^2 + P_1 + \rho g h_1 = \frac{1}{2}\rho {V_2}^2 + P_2 + \rho g h_2 \quad (1)$$

Point 1 is in the water tank and Point 2 is at the exit location where the water is about to injects out. In this system h_1 and h_2 are almost at the same level and V_1, P_2 may be equal to zero. Therefore, Eq. (1) can be rearranged as Eq. (2):

$$P_1 = \frac{1}{2}\rho {V_2}^2 \quad (2)$$

As it expected, a considerable energy will be lost at the micrometer bore nozzle. To find out about the relation between the waterjet velocity and its pressure, a calibration process was performed, and outcome illustrated in Fig. 1-a. It should be noted that according to Eq. (2) waterjet velocity for all nozzles should be the same as the equation is independent from nozzle's bore diameter. Furthermore, Fig. 1-b presents the outcome of waterjet velocity versus gage pressure for saturated saltwater (room temperature, NaCl, pressure $\cong$ 1 atm). Density of NaCl is 2.17 g/ml and its maximum solubility at 25 C° is 357 mg/ml of water. Therefore, density of saturated saltwater at room temperature is equal to 1.165 g/ml [27].

3. Experiments

3.1. Ethical statement

All tests carried in this study are performed on spinal cord harvested from freshly slaughtered sheep animal. The harvested samples are obtained from the same race and age. The samples were harvested considering the local ethical policy and approved standard for biological testing. Sample preparation and laboratory instruments were used for all the samples at the same lab conditions.

3.2. Test 1

This test is based on evaluation of the cutting uniformity in theta direction and along the spinal cord. Spinal cords of 50 sheep (same race, male, 47±2 kg weight, 2 years of old) are divided to 5 pieces (~ 5 cm long) and then mounted in a custom made fixture shown in Figs. 2 and 3. A high speed and resolution camera is used to monitor and record the event.

The first experiment performed and tested with a single nozzle (0.4 mm) with 4 bar pressure for 15 s. To check the repeatability and reliability of the recorded result, the test scenario is repeated for 10 times (anterior, posterior, and lateral view) with total 250 tests record. Nozzle is held normal to axis of spinal cord (90°) with 2 cm away from meninges layers to avoid waterjet splash. The experimental setup is illustrated in Fig. 3-i and Fig. 3-ii.

As mentioned, dura is the toughest layer of meninges and comprised of dense fibrous tissue and it is stiff enough to protect the spinal cord structure. As expected, waterjet is ricochet after interaction with sample without visible cutting penetration in this test.

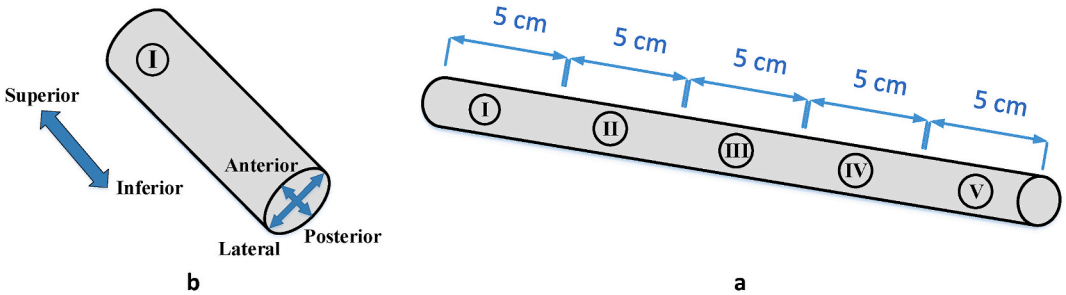

Fig. 2. Specimen sections preparationa) spinal cord divided to five pieces, b) section I ready to fix in fixture.

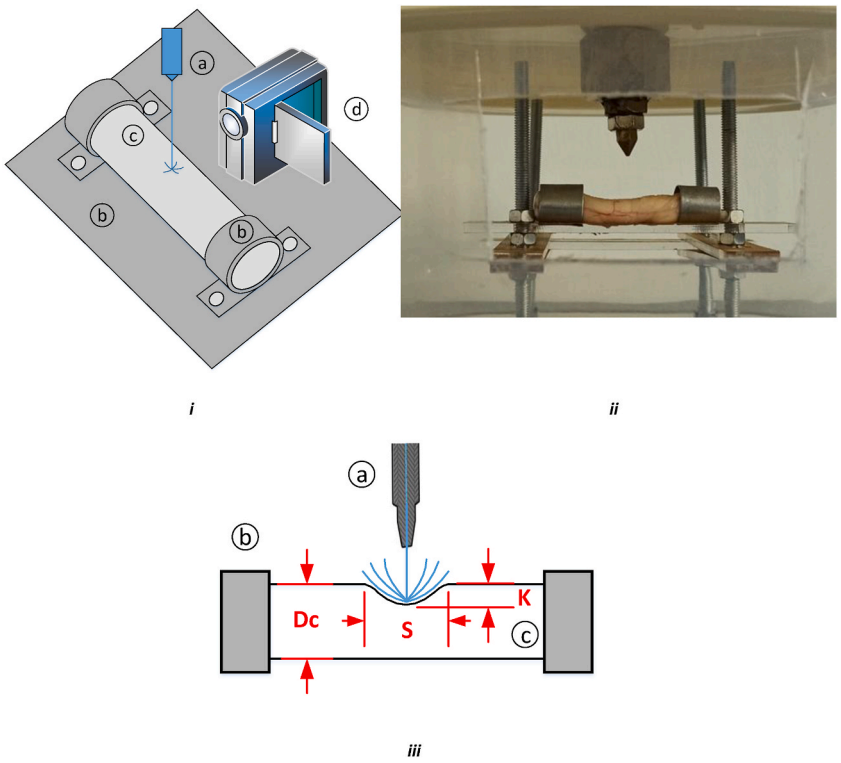

Fig. 3. i) schematic and ii) real view of specimen held in fixture, iii) defined parameters of test 1, a) nozzle b) fixture, c) specimen, d) camera.

Table 1
Defined parameters of test 1 for nozzle with diameter of 0.4 mm and 4 bar pressure.

Section No.		View					
		Anterior		Posterior		Lateral	
		K/*Dc*	*S*/*Dc*	*K*/*Dc*	*S*/*Dc*	*K*/*Dc*	*S*/*Dc*
I	Mean	0.157	0.625	0.167	0.639	0.163	0.613
	RMSE	6e-4	0.0517	13e-4	0.0815	6e-4	0.0611
	Variance	0.6 e−4	0.0052	1.3 e−4	0.0081	0.6 e−4	0.0061
	Stand. Deviation	0.008	0.0719	0.012	0.0903	0.008	0.0782
	Max-Min	0.028	0.2211	0.034	0.3421	0.028	0.2539
II	Mean	0.155	0.563	0.162	0.554	0.159	0.583
	RMSE	18e-4	0.0826	3e-4	0.0664	8e-4	0.1022
	Variance	1.8 e−4	0.0083	0.3 e−4	0.0066	0.8 e−4	0.0102
	Stand. Deviation	0.013	0.0909	0.006	0.0815	0.009	0.1011
	Max-Min	0.044	0.2728	0.019	0.2512	0.027	0.3366
III	Mean	0.161	0.583	0.157	0.623	0.163	0.570
	RMSE	14e-4	0.1342	6e-4	0.1015	7e-4	0.0277
	Variance	1.4 e−4	0.0134	0.6 e−4	0.0101	0.7 e−4	0.0028
	Stand. Deviation	0.012	0.1158	0.008	0.1007	0.008	0.0527
	Max-Min	0.038	0.4384	0.023	0.3797	0.028	0.1508
IV	Mean	0.158	0.582	0.162	0.602	0.156	0.580
	RMSE	16e-4	0.0599	6e-4	0.1042	15e-4	0.0629
	Variance	1.6 e−4	0.0060	0.6 e−4	0.0104	1.5 e−4	0.0063
	Stand. Deviation	0.012	0.0774	0.008	0.1021	0.012	0.0793
	Max-Min	0.045	0.2710	0.026	0.3441	0.036	0.2437
V	Mean	0.163	0.583	0.158	0.570	0.153	0.547
	RMSE	18e-4	0.0507	6e-4	0.1526	7e-4	0.0616
	Variance	1.8 e−4	0.0051	0.6 e−4	0.0153	0.7 e−4	0.0062
	Stand. Deviation	0.013	0.0712	0.008	0.1235	0.008	0.0785
	Max-Min	0.039	0.2241	0.027	0.5176	0.030	0.2484

Considering the outcome of this tests, two key parameters are defined to show deflection of meninges during and after the test. This is when the nozzle is held normal to the spinal cord sample, as illustrated in Fig. 3-iii. These parameters are measured by ImageMeter software and are presented in Table 1.

Table 1 illustrate the result of the first experiment. Deflection of spinal cord shown to be independent from the theta direction and longitudinal direction of the spinal cord. Therefore, to get a reasonable result, the samples behave in similar manner under waterjet. However, in continue, to get more accuracy on the results, the waterjet nozzle was fixed toward anterior side of the sample.

Parameters of K and S distributed in semi-Gaussian shape around mean value. For example, Fig. 4 shows distribution of $K/\ Dc$ for section I in anterior view around mean value of 0.157.

3.3. Test 2

In this test, effects of nozzle diameter and waterjet velocity on the spinal cord deflection is investigated. Moreover, the effect of fluid's density is studied by implementing two fluids with different densities ($\rho_1 \simeq 1000(kg/m^3)$ and $\rho_2 \simeq 1160(kg/m^3)$). It should be noted that small temperature variation of waterjet and sample during the test is neglected. For the purpose this test, 20 sheep spinal cord specimens are divided into 6 pieces (each 4 cm long) and mounted in a custom made rig as shown in Fig. 3. The samples are tested with different bore size nozzles (0.2, 0.3, 0.4, 0.5 mm in diameter) with a pressure of 1–8 bar pressure. Nozzle is located normal to spinal cord axis (90°) with 2 cm away from meninges layers to avoid waterjet splash.

Deflection of spinal cord are designated in Fig. 3 and presented in Table 2 and Table 3 as K and S undergoing 10 s waterjet process (T1) and 5 s after waterjet is discontinued (T2). The T2 measured to evaluate the plastic deflection of the sample after 5 s test. Each test repeated three times to improve ensure about the reliability of the recorded data.

As expected, dura shows to be stiff enough to protect spinal cord from rupture under waterjet pressure up to 8 bar for different nozzles. Even though, the scare of cutting is not appeared in dura mater under 8 bar waterjet pressure, there is no evidence to confirm that the internal tissue of the spinal cord is not damaged. As can be seen in Table 2, K/Dc is close to 0.3, with this deflection medical investigation is needed to study possible damages to internal tissue of spinal cord to develop a standard criteria for its failure under waterjet interaction. Also it is noticeable from Table 2 that no significant plastic deformation remains permanently on spinal cord up to 8 bar pressure. It means, if the temporary deflection not cause any damage on the internal tissues of spinal cord, then its structure returns to normal shape quickly.

Table 3 which is like Table 2 in term of output velocity and nozzle diameter, presents the effect of waterjet fluid density on spinal cord deformation. To maintain the same output velocity, a corresponding pressure should be calculated from the regression equations. Results of Table 3 in comparison with Table 2 indicate that fluid density plays an important role in deformation of spinal cord. As density of fluid increases, deflection parameters, K and S, increases.

As stated in the previous studies on spinal cord [8–12], findings show that waterjet is feasible and reliable option for surgeries in the vicinity of spinal cord. Characteristics of waterjet, like Tables 2 and 3, may help surgeons to have a successful surgery along with preservation of neurological function. Also 8 bar pressure of this waterjet could be a safe threshold to prevent spinal cord rupture during the surgery.

3.4. Test 4

In real surgical operation, the waterjet may not necessarily applies perpendicular to the spinal cord axis. In this test, effect of waterjet angle on spinal cord deflection is investigated.

In test 3 setup, 5 sheep spinal cords been divided into 6 pieces (each 4 cm long) and each carefully secured in the test rig as shown in Fig. 3.

All samples are tested with a nozzle (0.4 mm in diameter) with 4 bar pressure at three different angles (30°, 60°, 90°) and 2 cm away from spinal cord as illustrated in Fig. 5.

Deflection parameter of spinal cord (K) is measured after 10 s of the test. Data of each nozzle angle is collected after repeating the test five times.

Results show that maximum deformation happens when nozzle is normal to the spinal cord axis. In other words, the 90° is a critical angle of attack and can be considered as a criteria for damage prevention of spinal cord.

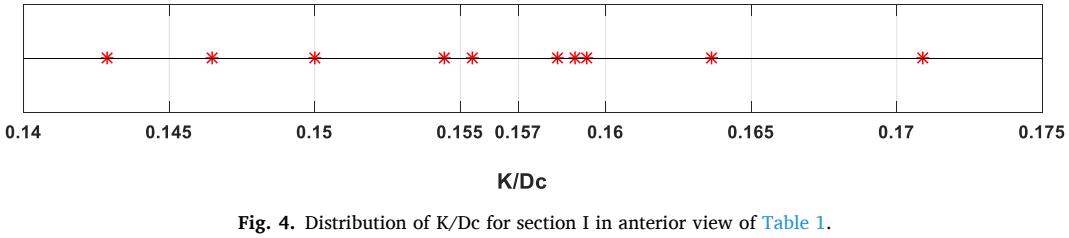

Fig. 4. Distribution of K/Dc for section I in anterior view of Table 1.

Table 2
Defined parameters of test 2 with fluid density of $\rho_1 \simeq 1000(\mathrm{kg}/\mathrm{m}^3)$, tenth seconds of test (T1) and 5 s after the test (T2).

P (bar)	V (m/s)	Parameters	Nozzle Diameter 0.2 mm – Pure Water			
			T1		T2	
			K/Dc	S/Dc	K/Dc	S/Dc
1	**11.6**	Mean	$\simeq 0$	$\simeq 0$	$\simeq 0$	$\simeq 0$
		Stand. deviation	–	–	–	–
2	**16.9**	Mean	$\simeq 0$	$\simeq 0$	$\simeq 0$	$\simeq 0$
		Stand. deviation	–	–	–	–
3	**22.5**	Mean	$\simeq 0$	$\simeq 0$	$\simeq 0$	$\simeq 0$
		Stand. deviation	–	–	–	–
4	**26.3**	Mean	0.050	0.233	$\simeq 0$	$\simeq 0$
		Stand. deviation	0.0056	0.021	–	–
5	**28.1**	Mean	0.055	0.261	$\simeq 0$	$\simeq 0$
		Stand. deviation	0.0385	0.029	–	–
6	**31.8**	Mean	0.061	0.288	$\simeq 0$	$\simeq 0$
		Stand. deviation	0.0043	0.023	–	–
7	**35**	Mean	0.066	0.312	$\simeq 0$	$\simeq 0$
		Stand. deviation	0.0053	0.031	–	–
8	**37**	Mean	0.070	0.323	0.05	0.3
		Stand. deviation	0.0084	0.025	–	–
P (bar)	V (m/s)	Parameters	Nozzle Diameter 0.3 mm – Pure Water			
			T1		T2	
			K/Dc	S/Dc	K/Dc	S/Dc
1	**6.3**	Mean	$\simeq 0$	$\simeq 0$	$\simeq 0$	$\simeq 0$
		Stand. deviation	–	–	–	–
2	**9.6**	Mean	$\simeq 0$	$\simeq 0$	$\simeq 0$	$\simeq 0$
		Stand. deviation	–	–	–	–
3	**12**	Mean	0.051	0.251	$\simeq 0$	$\simeq 0$
		Stand. deviation	0.0031	0.025	–	–
4	**13.5**	Mean	0.060	0.278	$\simeq 0$	$\simeq 0$
		Stand. deviation	0.0054	0.026	–	–
5	**15.4**	Mean	0.067	0.302	$\simeq 0$	$\simeq 0$
		Stand. deviation	0.0053	0.024	–	–
6	**17.7**	Mean	0.075	0.321	$\simeq 0$	$\simeq 0$
		Stand. deviation	0.0056	0.029	–	–
7	**19.1**	Mean	0.081	0.349	$\simeq 0$	$\simeq 0$
		Stand. deviation	0.0089	0.038	–	–
8	**20.6**	Mean	0.088	0.355	0.05	0.3
		Stand. deviation	0.0088	0.032	–	–
P (bar)	V (m/s)	Parameters	Nozzle Diameter 0.4 mm – Pure Water			
			T1		T2	
			K/Dc	S/Dc	K/Dc	S/Dc
1	**9.3**	Mean	0.074	0.341	$\simeq 0$	$\simeq 0$
		Stand. deviation	0.0067	0.037	–	–
2	**14.6**	Mean	0.109	0.453	$\simeq 0$	$\simeq 0$
		Stand. deviation	0.0087	0.041	–	–
3	**18.1**	Mean	0.136	0.556	$\simeq 0$	$\simeq 0$
		Stand. deviation	0.0068	0.044	–	–
4	**20.6**	Mean	0.160	0.644	$\simeq 0$	$\simeq 0$
		Stand. deviation	0.0161	0.071	–	–
5	**23.4**	Mean	0.181	0.727	$\simeq 0$	$\simeq 0$
		Stand. deviation	0.0127	0.073	–	–
6	**26.5**	Mean	0.200	0.805	$\simeq 0$	$\simeq 0$
		Stand. deviation	0.0120	0.072	–	–
7	**28.8**	Mean	0.218	0.871	0.05	0.4
		Stand. deviation	0.0174	0.061	–	–
8	**31**	Mean	0.235	0.923	0.08	0.4
		Stand. deviation	0.0117	0.074	–	–
P (bar)	V (m/s)	Parameters	Nozzle Diameter 0.5 mm – Pure Water			
			T1		T2	
			K/Dc	S/Dc	K/Dc	S/Dc
1	**7.7**	Mean	0.093	0.411	$\simeq 0$	$\simeq 0$
		Stand. deviation	0.0084	0.045	–	–
2	**12**	Mean	0.138	0.562	$\simeq 0$	$\simeq 0$
		Stand. deviation	0.0110	0.051	–	–
3	**15.2**	Mean	0.174	0.714	$\simeq 0$	$\simeq 0$
		Stand. deviation	0.0139	0.057	–	–
4	**17**	Mean	0.205	0.816	$\simeq 0$	$\simeq 0$
		Stand. deviation	0.0143	0.082	–	–

(*continued on next page*)

Table 2 (*continued*)

P (bar)	V (m/s)	Parameters	Nozzle Diameter 0.2 mm – Pure Water			
			T1		T2	
			K/Dc	S/Dc	K/Dc	S/Dc
5	**18.5**	Mean	0.232	0.924	$\simeq 0$	$\simeq 0$
		Stand. deviation	0.0234	0.065	–	–
6	**21.6**	Mean	0.258	1.017	0.05	0.3
		Stand. deviation	0.0155	0.081	–	–
7	**24**	Mean	0.282	1.096	0.08	0.4
		Stand. deviation	0.0141	0.098	–	–
8	**26**	Mean	0.304	1.159	0.10	0.4
		Stand. deviation	0.0212	0.116	–	–

Table 3
Defined parameters of test 2 with fluid density of $\rho_2 \simeq 1160(\mathrm{kg}/\mathrm{m}^3)$, tenth seconds of test (T1) and 5 s after the test (T2).

P (bar)	V (m/s)	Parameters	Nozzle Diameter 0.5 mm – Salt Water			
			T1		T2	
			K/Dc	S/Dc	K/Dc	S/Dc
1.2	**7.7**	Mean	0.095	0.354	$\simeq 0$	$\simeq 0$
		Stand. deviation	0.0059	0.028	–	–
2.5	**12**	Mean	0.145	0.546	$\simeq 0$	$\simeq 0$
		Stand. deviation	0.0115	0.038	–	
3.6	**15.2**	Mean	0.180	0.677	$\simeq 0$	$\simeq 0$
		Stand. deviation	0.0081	0.066	–	–
4.4	**17**	Mean	0.209	0.762	$\simeq 0$	$\simeq 0$
		Stand. deviation	0.0211	0.043	–	–
5.2	**18.5**	Mean	0.234	0.841	0.06	0.3
		Stand. deviation	0.0175	0.098	–	–
6.6	**21.6**	Mean	0.268	0.968	0.09	0.3
		Stand. deviation	0.0146	0.082	–	–
7.9	**24**	Mean	0.297	1.077	0.11	0.4
		Stand. deviation	0.0241	0.061	–	–
9.1	**26**	Mean	0.323	1.171	0.12	0.4
		Stand. deviation	0.0145	0.086	–	–

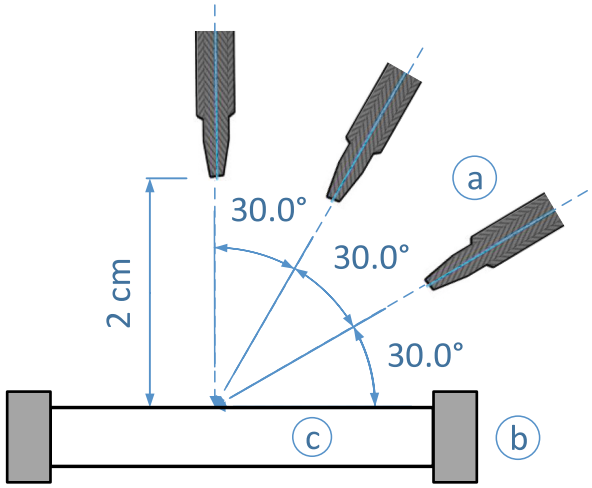

Fig. 5. interaction angels of waterjet and sample; a) nozzle b) fixture, c) specimen.

3.5. Test 4

Due to high stiffness of dura mater, it is shown that waterjet system cannot cut the spinal cord under the 8 bars pressure. So, the focus in this test is to investigate the interaction between waterjet beam and dura mater layer.

Zhang developed an in-vivo indentation test method to assess the equivalent Young's Modulus of sheep spinal cord with meninges.

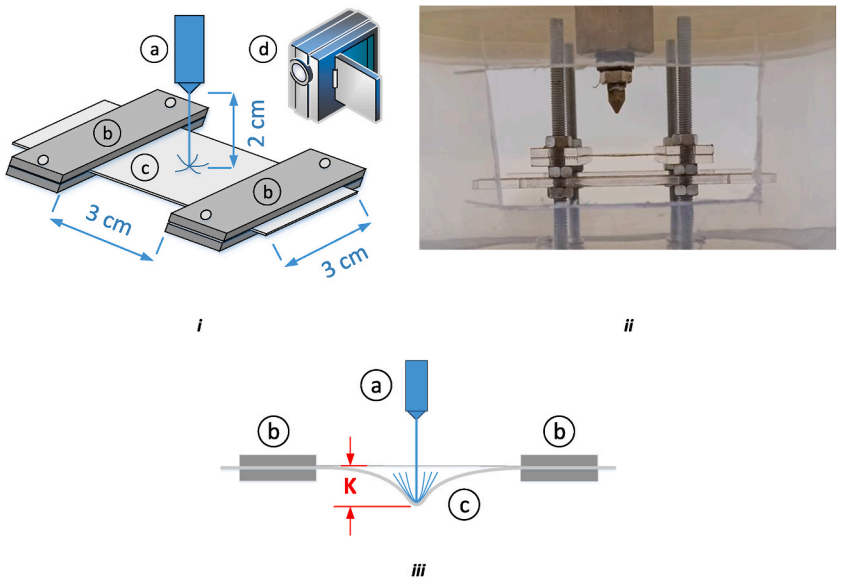

Fig. 6. i) schematic and ii) real view of dura mater layer held in the fixture, iii) defined parameter of test 4a) nozzle, b) fixture, c) specimen (dura mater), d) camera.

The proposed equivalent modulus had a mean of 0.022 MPa and a standard deviation of 0.014 MPa. As mentioned, the elastic modulus of spinal cord is much smaller than the elastic modulus of dura mater [26].

In this study 10 sheep spinal cord been divided into 4 pieces and their dura mater are removed. Then harvested dura layer (with approximate size of 5 cm*3 cm) is fixed in a test rig as shown in Fig. 6. The deformation of the sample under waterjet during the test is recorded with a high-speed camera. The samples are tested with different nozzle bore sizes (0.2, 0.3, 0.4, 0.5 mm in diameter) with pressure of 1–8 bar for each test. The nozzle located normal to dura mater layer at a distance of 2 cm away from dura layer. The temperature variation of waterjet and sample during the test is neglected. As shown in Fig. 6, K is defined to present effects of waterjet parameters on dura mater deflection.

Table 4 shows values of K for different waterjet velocity of all nozzles under a 10 s application of waterjet (T1) and 5 s after waterjet is discontinued (T2).

Results show that there is no visible damage was detected in dura mater under the waterjet up to 8 pressure with all nozzles (0.2–0.5 mm in diameter). Consequently, for the medical application, it may be claimed that there is no damage or significant permanent plastic deformation is predicted on dura mater under 8 bar waterjet pressure with any nozzle size.

4. Results and discussion

Resection of tumors and medical operation in the vicinity of spinal cord is complicated and risky, because the margins between tumors and spinal cord tissue are often unclear and irreversible damage to the spinal cord may occur. Nowadays, scientists are studying application of waterjet for removing of tumors to have more safe operation. In the present study, a system of waterjet is designed to perform sheep spinal cord because of its availability and similarity to the human spinal cord. Moreover, defining a criterion for waterjet to minimize its risk of damage to spinal cord during the surgical operation was the objective of this study. For this purpose, four group of tests are carried out.

Test 1 is designed to evaluate uniformity of spinal cord in theta direction and alongside the spinal cord. Two key parameters, K and S, are designated to illustrate deflection of spinal cord. Results show that these parameters are independent of the theta direction and selected sample along the spinal cord. It indicates all selected specimens behave in alike manner in interaction with waterjet. To improve the precision of the process, the waterjet is implemented to interact with anterior side of spinal cord.

Effects of fluid density and waterjet parameters on spinal cord deflection is investigated in Test 2. Prepared specimens are tested with pressure of 1–8 bar with all nozzles (0.2, 0.3, 0.4, 0.5 mm in diameter). Two deflection parameters, K and S, are measured in this test as well. Dura mater can protect spinal cord from rupture under waterjet pressure up to 8 bar, even different nozzle size is used. Although no visible damage and plastic deformation is perceived in this test, further investigation is needed to study possible damage to the internal tissue of spinal cord. Considering the result of current study, medical researchers do not have to test the spinal cord deformation in interaction with waterjet under 8 bars pressure.

Since the angle between waterjet and spinal cord axis is not always perpendicular in medical operation, effect of waterjet angle on spinal cord deflection is studied in Test 3. Samples are tested with a nozzle (0.4 mm) with 4 bar pressure at three different angles (30°, 60°, 90°). Deflection parameter of spinal cord (K) is presented for tenth seconds of the test. It is concluded from results that maximum deformation occurs while nozzle is normal to spinal cord. Indeed, determinative threshold for waterjet properties can be defined based

Table 4
Defined parameter of test 2 during and after the test, tenth seconds of test (T1) and 5 s after test (T2).

P (bar)	V (m/s)	Parameters	Nozzle Diameter 0.2 mm	
			T1	T2
			K/Dc	K/Dc
1	**11.6**	Mean	0.0926	$\simeq 0$
		Stand. deviation	0.0064	–
2	**16.9**	Mean	0.1156	$\simeq 0$
		Stand. deviation	0.0104	–
3	**22.5**	Mean	0.1334	$\simeq 0$
		Stand. deviation	0.0093	–
4	**26.3**	Mean	0.1485	$\simeq 0$
		Stand. deviation	0.0160	–
5	**28.1**	Mean	0.1619	$\simeq 0$
		Stand. deviation	0.0097	–
6	**31.8**	Mean	0.1741	$\simeq 0$
		Stand. deviation	0.0139	–
7	**35**	Mean	0.1854	$\simeq 0$
		Stand. deviation	0.0166	–
8	**37**	Mean	0.1959	0.05
		Stand. deviation	0.0137	–
P (bar)	V (m/s)	Parameters	Nozzle Diameter 0.3 mm	
			T1	T2
			K/Dc	K/Dc
1	**6.3**	Mean	0.1011	$\simeq 0$
		Stand. deviation	0.0101	–
2	**9.6**	Mean	0.1298	$\simeq 0$
		Stand. deviation	0.0116	–
3	**12**	Mean	0.1525	$\simeq 0$
		Stand. deviation	0.0091	–
4	**13.5**	Mean	0.1720	$\simeq 0$
		Stand. deviation	0.0137	–
5	**15.4**	Mean	0.1894	$\simeq 0$
		Stand. deviation	0.0170	–
6	**17.7**	Mean	0.2054	$\simeq 0$
		Stand. deviation	0.0143	–
7	**19.1**	Mean	0.2202	$\simeq 0$
		Stand. deviation	0.0132	–
8	**20.6**	Mean	0.2341	0.05
		Stand. deviation	0.0257	–
P (bar)	V (m/s)	Parameters	Nozzle Diameter 0.4 mm	
			T1	T2
			K/Dc	K/Dc
1	**9.3**	Mean	0.2542	$\simeq 0$
		Stand. deviation	0.0305	–
2	**14.6**	Mean	0.3312	$\simeq 0$
		Stand. deviation	0.0298	–
3	**18.1**	Mean	0.3920	$\simeq 0$
		Stand. deviation	0.0313	–
4	**20.6**	Mean	0.4443	$\simeq 0$
		Stand. deviation	0.0444	–
5	**23.4**	Mean	0.4910	$\simeq 0$
		Stand. deviation	0.0343	–
6	**26.5**	Mean	0.5337	$\simeq 0$
		Stand. deviation	0.0426	–
7	**28.8**	Mean	0.5733	0.05
		Stand. deviation	0.0515	–
8	**31**	Mean	0.6105	0.08
		Stand. deviation	0.0427	–
P (bar)	V (m/s)	Parameters	Nozzle Diameter 0.5 mm	
			T1	T2
			K/Dc	K/Dc
1	**7.7**	Mean	0.3057	$\simeq 0$
		Stand. deviation	0.0244	–
2	**12**	Mean	0.4055	$\simeq 0$
		Stand. deviation	0.0365	–
3	**15.2**	Mean	0.4849	$\simeq 0$
		Stand. deviation	0.0339	–
4	**17**	Mean	0.5535	$\simeq 0$
		Stand. deviation	0.0498	–

(*continued on next page*)

Table 4 (*continued*)

P (bar)	V (m/s)	Parameters	Nozzle Diameter 0.2 mm	
			T1	T2
			K/Dc	K/Dc
5	**18.5**	Mean	0.6150	$\simeq 0$
		Stand. deviation	0.0676	–
6	**21.6**	Mean	0.6714	0.05
		Stand. deviation	0.0470	–
7	**24**	Mean	0.7239	0.08
		Stand. deviation	0.0434	
8	**26**	Mean	0.7732	0.10
		Stand. deviation	0.0387	–

on 90° attack angle.

Results of the first three tests show that dura mater prevents any obvious damage to the spinal cord under 8 bar waterjet pressure with the choice of different nozzle sizes. Test 4 analyzed durra mater deformation under waterjet reaction. Dura mater specimens are tested with nozzles (0.2, 0.3, 0.4, 0.5 mm in diameter) with pressure of 1–8 bar for each test and K value is measured to show deflection of dura mater at T1 and T2. As can be expected, in this test no damage and considerable plastic deformation is observed on dura mater layer in interaction with waterjet under 8 bar pressure with all tested nozzle sizes.

5. Conclusion

In this study a system of waterjet is designed to investigate the interaction of waterjet and spinal cord to define a safe operational criterion. For this purpose, effect of three parameters namely; waterjet density, waterjet velocity and nozzle diameter, on failure criteria of spinal cord surgery is investigated.

Results show that dura mater is stiff enough to protect spinal cord against any rupture from waterjet pressure under 8 bars disregard its nozzle size when waterjet is normal to spinal cord. Spinal cord would behave purely elastic in this range of pressure. No visible damage is occurred on dura mater layer, while it cannot be guaranteed that the internal tissue of the spinal cord is not degraded under the pressure. In this regards, three key parameters of deformation in spinal cord are defined as depth and span of spinal cord deformation and dura mater deflection. These parameters play the key role in achieving the standard threshold criteria for safe medical operation of spinal cords.

Effect of angle between waterjet and spinal cord on spinal cord deflection is investigated. It should be noted that the maximum deflection takes place when waterjet flow is normal to the spinal cord. Variation of dura mater under the waterjet is also studied. Results show that interaction of waterjet do not damage the dura mater anyway.

Declaration of competing interest

The authors declare no competing interests.

References

[1] A. Maton, H. Jean, W.M. Charles, J. Susan, Q.W. Maryanna, L. David, D.W. Jill, Human Biology and Health, 1 ed., Prentice Hall, Englewood Cliffs, New Jersey, USA, 1993.
[2] P.A. Guertin, Central pattern generator for locomotion: anatomical, physiological, and pathophysiological considerations, Front. Neurol. 3 (2013) 183, https://doi.org/10.3389/fneur.2012.00183.
[3] Vasković, J., Ventricles, meninges and blood vessels of the brain. Retrieved from KENHUB: https://www.kenhub.com/en/library/anatomy/meninges-of-the-brain-and-spinal-cord. Accessed December 21, 2021.
[4] L. Benowitz, Y. Yin, Optic nerve regeneration, Arch. Ophthalmol. 128 (8) (2010) 1059–1064, https://doi.org/10.1001/archophthalmol.2010.152.
[5] M. Setzer, R.D. Murtagh, F.R. Murtagh, et al., Diffusion tensor imaging tractography in patients with intramedullary tumors: comparison with intraoperative findings and value for prediction of tumor resectability, J. Neurosurg. Spine 13 (3) (2010) 371–380, https://doi.org/10.3171/2010.3.SPINE09399.
[6] Y. Ogawa, A. Nakagawa, K. Takayama, T. Tominaga, Pulsed laser-induced liquid jet for skull base tumor removal with vascular preservation through the transsphenoidal approach: a clinical investigation, Acta Neurochir. 153 (4) (2011) 823–830, https://doi.org/10.1007/s00701-010-0925-x.
[7] A. Nakagawa, Pulsed laser-induced liquid jet system for treatment of sellar and parasellar tumors: safety evaluation, J. Neurol. Surg. Cent. Eur. Neurosurg. 76 (6) (2015) 473–482, https://doi.org/10.1055/s-0034-1396436.
[8] T. Endo, A. Nakagawa, T. Tominaga, A new application of Piezo actuator-driven pulsed waterjet in dissecting the spinal cord. An experimental study of Swine, Trans. Jpn. Soc. Med. Biol. Eng. 52 (2014), https://doi.org/10.11239/jsmbe.52.O-65. O-65.
[9] T. Endo, Y. Takahashi, A. Nakagawa, K. Niizuma, M. Fujimura, T. Tominaga, Use of actuator-driven pulsed water jet in brain and spinal cord cavernous malformations resection, Operative Neurosurgery 11 (3) (2015) 394–403, https://doi.org/10.1227/NEU.0000000000000867.
[10] T. Endo, J. Wenting, A. Nakagawa, H. Endo, Y. Sagae, M. Iwasaki, T. Tominaga, New application of actuator-driven pulsed water jet for spinal cord dissection: an experimental study in pigs, J. Neurol. Surg. Cent. Eur. Neurosurg. 78 (2) (2017 Mar) 137–143, https://doi.org/10.1055/s-0036-1584919.
[11] N. Balak, Quadrantectomy for resection of spinal ependymomas with a new classification of unilateral approaches regarding bone drilling and the use of a new tool: the Balak ball-tipped water jet dissector, Interdisciplinary Neurosurgery 5 (2016) 18–25, https://doi.org/10.1016/j.inat.2016.03.002.
[12] A.H. Alamoud, E. Baillot, C. Belabbas, H.S. Samimi Ardestani, H. Bahai, A. Baldit, et al., Continuous and pulsed experiments with numerical simulation to dissect pituitary gland tumour by using liquid jet, Eng. Lett. 25 (3) (2017) 348–353.
[13] R.B. Ashman, J.E. Bechtold, W.T. Edwards, C.E. Johnston, P.C. McAfee, A.F. Tencer, In vitro spinal arthrodesis implant mechanical testing protocols, J. Spinal Disord. 2 (4) (1989) 274–281.

[14] S.J. Edmondston, K.P. Singer, R.E. Day, P.D. Breidahl, R.I. Price, Formalin fixation effects on vertebral bone density and failure mechanics: an study of human and sheep vertebrae, Clin. BioMech. 9 (3) (1994) 175–179, https://doi.org/10.1016/0268-0033(94)90018-3.
[15] S. Eggli, F. Schläpfer, M. Angst, P. Witschger, M. Aebi, Biomechanical testing of three newly developed transpedicular multisegmental fixation systems, Eur. Spine J. 1 (2) (1992) 109–116, https://doi.org/10.1007/BF00300937.
[16] G.S. Gurwitz, J.M. Dawson, M.J. McNamara, C.F. Federspiel, D.M. Spengler, Biomechanical analysis of three surgical approaches for lumbar burst fractures using short-segment instrumentation, .18, 977-982, Spine 18 (8) (1993) 977–982, https://doi.org/10.1097/00007632-199306150-00005.
[17] R. Gunzburg, R.D. Fraser, R. Moore, B. Vernon-Roberts, An experimental study comparing percutaneous discectomy with chemonucleolysis, Spine 18 (2) (1993) 218–226, https://doi.org/10.1097/00007632-199302000-00008.
[18] R.J. Moore, O.L. Osti, B. Vernon-Roberts, R.D. Fraser, Changes in endplate vascularity after an outer anulus tear in the sheep, Spine 17 (8) (1992) 874–878, https://doi.org/10.1097/00007632-199208000-00003.
[19] O.L. Osti, B. Vernon-Roberts, R.D. Fraser, Anulus tears and intervertebral disc degeneration. An experimental study using an animal model, Spine 15 (8) (1990) 762–767, https://doi.org/10.1097/00007632-199008010-00005.
[20] B. Ahlgren, A. Vasavada, R. Brower, C. Lydon, H. Herkowitz, M. Panjabi, Anular incision technique on the strength and multidirectional flexibility of the healing intervertebral disc, Spine 19 (8) (1994) 948–954, https://doi.org/10.1097/00007632-199404150-00014.
[21] D.A. Nagel, P.C. Kramers, B.A. Rahn, J. Cordey, S.M. Perren, A paradigm of delayed union and nonunion in the lumbosacral joint—a study of motion and bone grafting of the lumbosacral spine in sheep, Spine 16 (1991) 553–559, https://doi.org/10.1097/00007632-199105000-00012.
[22] R. Slater, D. Nagel, R.L. Smith, Biochemistry of fusion mass consolidation in the sheep spine, J. Orthop. Res. 6 (1) (1988) 138–144.
[23] T. Yamamuro, J. Shikata, H. Okumura, Replacement of the lumbar vertebrae of sheep with ceramic prostheses, J. Bone Joint Surg. 72 (5) (1990) 889–893, https://doi.org/10.1302/0301-620X.72B5.2211778.
[24] P. Vazquez-Seoane, J. Yoo, D. Zou, et al., Interference screw fixation of cervical grafts—a combined in vitro biomechanical and in vivo animal study, Spine 18 (8) (1993) 946–954, https://doi.org/10.1097/00007632-199306150-00002.
[25] H.J. Wilke, A. Kettler, K.H. Wenger, L.E. Claes, Anatomy of the sheep spine and its comparison to the human spine (199704)247:4<542::AID-AR13>3.0.CO;2, Anat. Rec. 247 (4) (1997), https://doi.org/10.1002/(SICI)1097-0185.
[26] H. Zhang, P. Falkner, Ch Cai, In-vivo indentation testing of sheep spinal cord with meninges, Mechanics of Biological Systems and Materials 6 (2016) 99–104, https://doi.org/10.1007/978-3-319-21455-9_11.
[27] W. Haynes, CRC Handbook of Chemistry and Physics, 94 ed., CRC Press, Taylor & Francis Group, Florida: Boca Raton, Florida, 2013-2014.